Original article

JOURNAL OF REINFORCED PLASTICS & COMPOSITES

Journal of Reinforced Plastics and Composites
2019, Vol. 38(21–22) 1014–1028

DOI: 10.1177/0731684419858708
journals.sagepub.com/home/jrp
SAGE

New models for estimating compressive strength of concrete confined with FRP sheets in circular sections

Yaser Moodi, Seyed Roohollah Mousavi and Mohammad Reza Sohrabi

Abstract

Models for determining the compressive strength of concrete columns confined by FRP have been presented in previous studies. In this study, a large set of experimental data regarding circular columns confined with different types of FRP has been collected. In order to increase the accuracy in the existing models, three modified models for predicting the compressive strength of circular columns confined with FRP has been proposed by using the collected data. The FRP strain efficiency factor in the proposed models is considered as: (i) a function of the strain ratio, (ii) a function of the confinement stiffness ratio, and (iii) a function of the combination of these ratios. Studying the analytical results using the proposed factors revealed that models wherein the FRP strain efficiency factor is a function of the strain ratio or the combination of the confinement stiffness ratio and strain ratio give results closer to the experimental results.

Keywords

Concrete, confinement, fiber reinforced polymers, compressive strength, circular section

Introduction

Confinement is an effective method for increasing the compressive strength of concrete columns. Concrete and steel jackets, still in common use today, were widely used in the past to reinforce concrete columns. Although these methods increase the structure's load bearing capacity, concrete jackets increase column section dimensions significantly and steel jackets perform weakly against adverse environmental conditions. Hence, older methods are to be replaced by innovative retrofitting systems which are economical and easy to implement.[1]

The idea of using FRP to reinforce the existing RC columns against seismic loads was first proposed in the mid-80s.[2] The 1990 (California) and 1995 (Kobe, Japan) earthquakes were important and effective factors for an extensive investigation regarding the application of FRP for the retrofitting of concrete and masonry structures in seismic zones.[3]

The first experimental study on concrete specimens confined with three types of FRP under axial compressive loads has been carried out by Nanni and Bradford.[4] They showed that the two mechanical properties of concrete, i.e. compressive strength and ductility, would increase by confining the specimens using FRP sheets.

Experimental studies that have examined the behavior of FRP-confined columns are many and models that have used these experimental results to estimate the concrete compressive strength are numerous. Fardis and Khalili[5] were the first to propose one of such models. Mander et al.[6] presented a model for estimating the compressive strength and axial strain of FRP-confined concrete. The result of their research was latter used by ACI 440.2R-02 Code.[7] To estimate the compressive strength of FRP-confined columns, many models have been proposed wherein the actual hoop rupture strain of the FRP wrap is not considered and their developments are based on the ultimate FRP strain reported by the manufacturer or on the Coupon

Civil Engineering Department, University of Sistan and Baluchestan, Zahedan, Islamic Republic of Iran

Corresponding author:
Seyed Roohollah Mousavi, University of Sistan and Baluchestan, Daneshgah Street, Zahedan 98155-987, Islamic Republic of Iran.
Email: s.r.mousavi@eng.usb.ac.ir

test. Lam and Teng[8] have considered a constant FRP strain efficiency factor (defined as the ratio of actual hoop rupture strain to ultimate tensile strain) for each FRP type. Sadeghian and Fam[9] have considered the maximum confinement stress in the "confinement stiffness ratio" as well as in "strain ratio" factors to take into account the actual rupture strain and have proposed some models to estimate the compressive strength of concrete cylinders confined with FRP by analyzing 518 specimens. Moodi et al.[10,11] proposed a model for estimating compressive strength of rectangular and square columns confined by FRP sheet. In their study, the effective strain coefficient of FRP was considered as function of shape section.

In this study, a large set of experimental data has been collected for circular columns confined with different types of FRP. Since modeling with larger statistical populations will lead to more reliable results, the statistical population used in this study is larger than those used in previous studies. FRP strain efficiency factor was considered as a factor of "strain ratio", "effective stiffness ratio", or their combination and three models were presented to estimate the compressive strength of circular, FRP-confined, concrete columns. Analyses of the results of 732 specimens show that the proposed models estimate the strength values more accurately.

Confinement mechanism

When concrete undergoes axial compression, it dilates laterally (volumetric expansion or dilation). This dilation is controlled by FRP jackets tensioned in loop directions. Figure 1 shows the confinement effects in the FRP-confined concrete. Neglecting tangential stresses in the longitudinal direction of the column specimen and considering the equilibrium of the stresses applied on the FRP, the actual maximum confining pressure ($f_{l,a}$) can be found as follows

$$f_{l,a} = \frac{2\,t_j f_{frp}}{D} = \frac{2E_{frp}\varepsilon_{h,rup}t_j}{D} \tag{1}$$

where D is the specimen diameter, E_{frp} is the elastic modulus of FRP material, t_j is the thickness of FRP wrap, and $\varepsilon_{h,rup}$ is the actual FRP rupture strain in loop directions defined as follows

$$\varepsilon_{h,rup} = k_\varepsilon \varepsilon_{frp} \tag{2}$$

where ε_{frp} is the ultimate tensile strain of FRP materials and k_ε is the strain efficiency factor. In most models presented for estimating the compressive strength of FRP-confined columns, actual FRP rupture strain

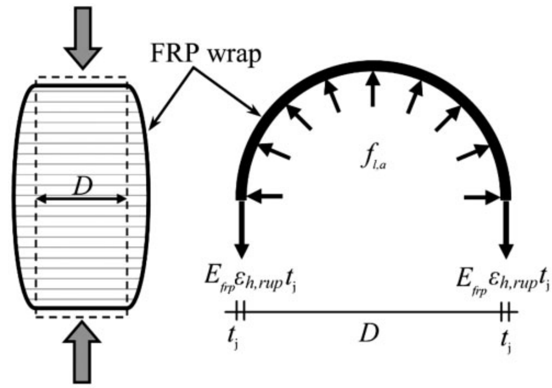

Figure 1. Confinement mechanism in concrete.[9]

has not been considered meaning that k_ε equals 1 in these models, but in some past studies,[8,9,12] the effect of this rupture strain has been considered. Lam and Tang[8] have considered a constant value for the strain factor for each types of FRP; for AFRP, CFRP, GFRP, and HM-CFRP, this factor is 0.851, 0.586, 0.624, and 0.788, respectively. Lim and Ozbakkaloglu[12] have presented a relationship for this factor in the form of the product of the following three factors:

1. Strain localization factor that considers the effect of non-uniform strain distribution in FRP.
2. Local (in-situ) factor that considers the effect of the difference between maximum strain measured on the column and that found from Coupon (flat tension) test.
3. FRP-to-fiber strain ratio.

They proposed equation (3) for strain efficiency factor as follows[12]

$$k_\varepsilon = 0.9 - 2.3f'_c \times 10^{-3} - 0.75E_{frp} \times 10^{-9} \tag{3}$$

where f'_c is the strength of unconfined concrete.

Sadeghian and Fam[9] proposed equation (4) as follows for FRP confinement stress considering the actual FRP rupture strain

$$f_{l,a} = \rho_\varepsilon \rho_k f'_c \tag{4}$$

where ρ_ε and ρ_k are the strain and effective stiffness ratio factors, respectively, defined as follows

$$\rho_k = \frac{2E_{frp}t_j}{(\frac{f'_c}{\varepsilon_{co}})D} \tag{5}$$

$$\rho_\varepsilon = \frac{\varepsilon_{h,rup}}{\varepsilon_{co}} \tag{6}$$

where ε_{co} is the strain related to f'_c in the unconfined concrete.

The FRP strain efficiency factor in this study has been considered as: (1) ratio of the ultimate FRP tensile strain to the strain related to f'_c and (2) ratio of the effective stiffness which is defined as the ratio of FRP elasticity modulus to the compressive strength of the unconfined concrete. More information will be provided in Section of compressive strength of confined concrete.

Experimental database

Tests performed on the FRP-confined concrete are numerous. In this study, a statistical population of 662 FRP-confined circular concrete specimens, extracted from various studies, has been used for modeling. The statistical population used in this study is more complete than those used in earlier researches and details of the specimens are given in Table 1. They have diameters of 47–406 mm (average 155 mm) and unconfined compressive strengths of 2.6–55.2 MPa (average 35 MPa). FRP types used in these database include CFRP, AFRP, GFRP, and HM-CFRP with moduli of elasticity ranging from 4.9 to 640 GPa (average 170 GPa) and ultimate tensile strength of 75–4810 MPa (average 2712 MPa). All FRP jackets used in these data are single direction (hoop direction). These experimental data will be used for formulation purposes.

Genetic algorithm

Optimization of structures has always been a noticeable developing area of research in the field of engineering optimization and has made highly progress in the last decade.[96,97]

The natural selection and evaluation process was first observed and documented by Charles Darwin. The fittest's survival philosophy makes it easier to reach the globally optimal solution. The methodology is implemented numerically and developed for optimization problems, where the mathematical use of GAs simulates natural evaluation and adaptation to environmental variation. The process is initiated by randomly or heuristically selecting a number of candidate design variables to create an initial population, which is then encouraged to evolve over generations to produce new designs that are better or fitter. It is necessary to device a genetic coding system for representation of design variable, which can be considered to be a direct analogy of DNA structure of chromosomes.

The design variables are coded by a bit string. With this binary representation, the design variables can be

Table 1. Summary of FRP-confined square and rectangular concrete specimens for modeling procedure.

Reference	Total number of database	Diameter (mm)	Unconfined concrete strength range (MPa)	FRP type	Reference	Total number of database	Diameter (mm)	Unconfined concrete strength range (MPa)	FRP type
Nanni and Bradford[4]	17	150	35.6–36.3	AFRP, GFRP	Karabinis and Rousakis[54]	16	200	35.7–38.5	CFRP
Ahmad et al.[13]	2	102	39.0–50.5	GFRP	Karam and Tabbra[55]	2	150	12.8	CFRP
Aire et al.[14]	6	150	42	CFRP, GFRP	Karantzikis et al.[56]	1	200	12.1	CFRP
Akogbe et al.[15]	12	100–300	21.7–26.5	CFRP	Karbhari and Gao[57]	3	152	38.4	CFRP
Al-Salloum[16]	2	150	32.4–36.2	CFRP	Kono et al.[58]	15	100	32.3–34.8	CFRP
Au and Buykozturk[17]	1	150	24.2	GFRP	Lam and Teng[59]	18	152	34.3–38.5	CFRP, GFRP
Benzaid et al.[18]	4	160	25.9–49.5	CFRP	Lam et al.[60]	6	152–152.5	38.9–41.1	CFRP
Berthet et al.[19]	42	160	25.0–52.0	CFRP, GFRP	Lee et al.[61]	5	150	36.2	CFRP
Bisby et al.[20]	3	150	34.4	CFRP	Dai et al.[62]	9	152	39.2	AFRP
Bisby et al.[21]	3	100	28	CFRP	Demers and Neale[63]	8	152	32.2–43.7	CFRP, GFRP
Bullo[22]	12	150	32.5	GFRP, HM-CFRP	Elsanadedy et al.[64]	6	50–150	41.1–53.8	CFRP
Carnpione et al.[23]	1	100	20.1	CFRP	Erdil et al.[65]	2	150	11.1–20.8	CFRP
Carey and Harries[24]	2	152–254	33.5–38.9	CFRP	Evans et al.[66]	1	150	37.3	CFRP

(continued)

Table 1. Continued

Reference	Total number of database	Diameter (mm)	Unconfined concrete strength range (MPa)	FRP type	Reference	Total number of database	Diameter (mm)	Unconfined concrete strength range (MPa)	FRP type
Comert et al.[25]	2	150	39	GFRP	Green et al.[67]	3	152	46.0–54.0	CFRP, GFRP
Cui and Sheikh[26]	24	152	45.6–48.1	CFRP, GFRP, HM-CFRP	Harmon and Slattery[68]	4	51	41	CFRP
Hosotani et al.[27]	2	200	41.7	CFRP, HM-CFRP	Harries and Carey[69]	2	152	31.8	CFRP
Iliki et al.[28]	5	150	32	CFRP	Harries and Kharel[70]	10	152	32.1	CFRP, GFRP
Issa[29]	3	150	23.6–23.9	CFRP	Matthys et al.[71]	2	150	34.9	CFRP, HM-CFRP
Rochette and Labossière[30]	7	100–150	42.0–43.0	CFRP, AFRP	Micelli et al.[72]	2	102	32.0–37.0	CFRP, GFRP
Jiang and Teng[31]	8	152	33.1–45.9	GFRP	Mirmiran et al.[73]	13	152.5	29.8–31.2	GFRP
Miyauchi et al.[32]	10	100–150	31.2–51.9	CFRP	Shehata et al.[74]	4	150	25.6–29.8	CFRP
Modarelli et al.[33]	3	150	28.4–38.2	CFRP, GFRP	Shehata et al.[75]	4	150–225	34	CFRP
Ongpeng[34]	2	180	27	CFRP	Silva and Rodrigues[76]	7	150–250	29.6–31.2	GFRP
Owen[35]	8	102–152	47.9–53.0	CFRP	Smith et al.[77]	4	250	35	CFRP
Ozbakkaloglu and Akin[36]	4	152	39	AFRP	Song et al.[78]	12	100–150	22.4	CFRP
Picher et al.[37]	1	152	39.7	CFRP	Stanton and Owen[79]	5	152.5	49	CFRP
Piekarcky et al.[38]	2	47	55	CFRP	Suter and Pinzelli[80]	16	150	33.3–54.0	CFRP, AFRP, GFRP, HM-CFRP
Valdmanis et al.[39]	6	150	40.0–44.3	CFRP	Tamuzs et al.[81]	4	150	20.8–48.8	CFRP
Li et al.[40]	1	152.4	45.6	GFRP	Teng et al.[82]	6	152.5	39.6	GFRP
Liang et al.[41]	12	100	22.7–25.9	CFRP	Theriault et al.[83]	5	51–304	18.0–37.0	CFRP, GFRP
Lin and Liao[42]	27	100–150	17.7–25.9	CFRP	Vincent and Ozbakkaloglu[84]	6	152	35.5–38.0	CFRP
Mandal et al.[43]	9	102–105	30.7–54.5	CFRP, GFRP	Wang and Wu[85]	12	150	30.9–52.1	CFRP
Mastrapa[44]	6	152.5	29.8–37.2	GFRP	Wang and Wu[86]	18	70–194	24.0–51.6	AFRP
Rousakis[45]	20	150	25.2–51.8	HM-CFRP	Wu and Jiang[87]	34	150	20.6–36.7	CFRP
Rousakis et al.[46]	6	150	20.4–49.2	CFRP	Wang and Zhang[88]	2	150	47.3–51.1	AFRP
Saenz and Pantelides[47]	4	152	40.3–47.5	CFRP	Watanabe et al.[89]	9	100	30.2	CFRP, AFRP, HM-CFRP
Santaros et al.[48]	3	150	15.3–28.1	CFRP	Wong et al.[90]	4	152.5	36.5–46.7	GFRP
Shahawy et al.[49]	9	152.5	19.4–49.0	CFRP	Wu and Jiang[91]	4	150	28.7–30.1	CFRP
Shao et al.[50]	2	152	40.2	GFRP	Wu et al.[92]	4	150	23	CFRP, AFRP, GFRP, HM-CFRP
Wu et al.[51]	10	150	23.1	CFRP, AFRP, GFRP, HM-CFRP	Yan et al.[93]	1	305	15.2	CFRP
Wu et al.[52]	2	100	46.4	AFRP	Youssef et al.[94]	40	152–406	29.4–44.6	CFRP, GFRP
Xiao and Wu[53]	27	152	33.7–55.2	CFRP	Zhang et al.[95]	1	150	34.3	CFRP

coded only as integers. So it is usually necessary to introduce a linear scaling conversion system to appropriately obtain the required range of parameter values. For example, a design having two continuous variables β_1 and β_2 each is coded as a fixed length 10 bit string like β_1=1001000011, β_2=1101010110. Values of these parameters are selected at random. A 10 bit string is employed with regard to the precision with which the variables should be represented. Total design is represented by a 20 bit string created simply by concatenating β_1 with β_2.

By doing so, it is possible to create a founding population with members each represented by a 20 bit string. The next stage of the procedure, following the specification of the initial design population, is that of reproduction, which incorporates the concept of natural selection. The fitness of different members of the population must be evaluated before mating to produce the next generation. The fitness F is computed from the objective function of the chosen problem accordingly.

The selection of mating pairs for reproduction is a crucial step in GA. There are two methods of mating pool selection: fitness proportional or roulette wheel (*RW*) and tournament selection (*TS*). The latter method is proved to provide good selective pressure by holding a tournament competition among $N = 2$ individuals. The best individual (winner) from this tournament is one with highest fitness and the winner is then inserted into the mating pool. The tournament competition continues until the mating pool is filled to generate new offspring. The tournament winners' mating pool has a single average fitness.

In biological reproduction, the child's chromosomal pattern is derived from the two parents' chromosomal strings and thus the child inherits both characteristics. In GA, it is the crossover process that ensures the transfer of design information from generation to generation, essentially by a simple swapping of one (single-point) or two sections (two-point) of bit string representation of two parent designs to obtain two offspring design solutions.

The positioning and extent of the crossover time is randomly selected and may differ in each generation for each mating couple. Following the crossover, the natural evolution of the mutation concept is introduced into GA by occasionally switching the bit value at a randomly selected location of the generated strings. This action is important as it protects against premature design convergence to an optimal solution. The procedure is repeated until according to the objective function the new generation ceases to improve. When this happens, the youngest generation's most fitting individual is an optimal design solution. Figure 2 shows sketch of the GA used in this work.[98]

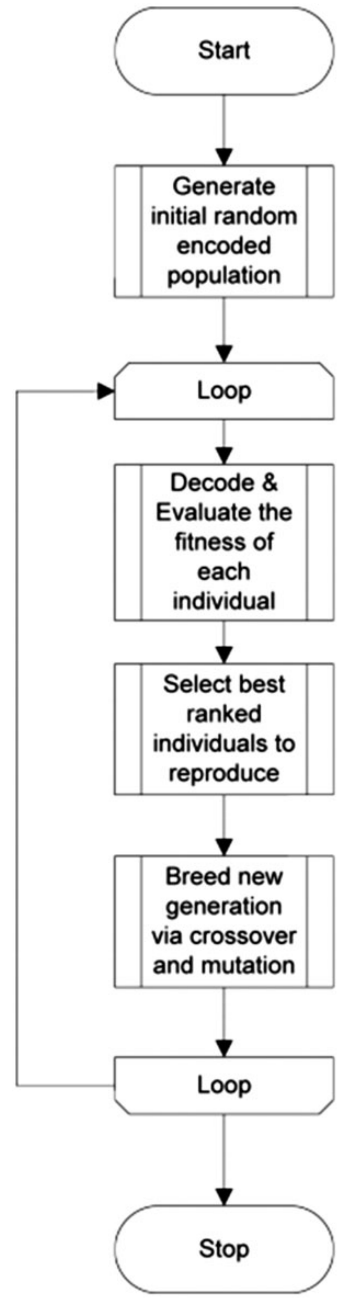

Figure 2. Sketch of the GA.[99]

In this study, GA is used for optimizing target function defined in the following sections. For all cases, initial population and iteration are considered 10,000 and 100, respectively.

Compressive strength of confined concrete

Compressive strength of FRP-confined concrete can be estimated by various models some of which are provided in Table 2. As shown, effects of actual FRP rupture

Table 2. Some of the available models for the compressive strength prediction of FRP-confined circular concrete columns.

Paper	Model	Descript
Wu and Wei[100]	$f'_{cc} = f'_c\left(0.75 + 2.7\left(\frac{f_l}{f'_c}\right)^{0.9}\right)$	$f_l = \frac{2f_{frp}t_j}{D}$
Pham and Hadi[101]	$f'_{cc} = 0.7f'_c + 1.8f_l + 5.7\frac{t}{D} + 13$	$f_l = \frac{2f_{frp}t_j}{D}$
Ozbakkaloglu and Lim[104]	$f'_{cc} = (1 + 0.0058\frac{k_1}{f'_c})f'_c + k_1(f_{l,a} - f_{lo})$	$f_{lo} = k_1\left(0.43 + 0.009\frac{k_1}{f'_c}\right)\varepsilon_{co}$ $k_1 = \frac{2E_{frp}t_j}{D} \geq f'^{1.65}_c$ $f_{l,a} = \frac{2E_{frp}\varepsilon_{h,rup}t_j}{D}$
Fahmy and Wu[102]	$f'_{cc} = f'_c + k_1 f_l$	$f_l = \frac{2f_{frp}t_j}{D}$ $\begin{cases} k_1 = 4.5 f_{l,a}^{-0.3} & f'_c \leq 40\,\text{MPa} \\ k_1 = 3.75 f_{l,a}^{-0.3} & f'_c > 40\,\text{MPa} \end{cases}$
Teng et al.[105]	$\begin{cases} f'_{cc} = f'_c(1 + 3.5(\rho_k - 0.01)\rho_\varepsilon & \rho_k \geq 0.01 \\ f'_{cc} = f'_c & \rho_k < 0.01 \end{cases}$	$\rho_k = \frac{2E_{frp}t_j}{\left(\frac{f'_c}{\varepsilon_{co}}\right)D}, \quad \rho_\varepsilon = \frac{\varepsilon_{h,rup}}{\varepsilon_{co}}$
Youssef et al.[94]	$f'_{cc} = f'_c(1 + 2.25(\frac{f_l}{f'_c})^{\frac{5}{4}})$	$f_l = \frac{2f_{frp}t_j}{D}$
Kumutha et al.[103]	$f'_{cc} = f'_c + 0.93f_l$	$f_l = \frac{2f_{frp}t_j}{D}$
Guralnick and Gunawan[106]	$f'_{cc} = f'_c(0.616 + \frac{f_{l,a}}{f'_c} + 1.57\sqrt{\frac{f_{l,a}}{f'_c} + 0.06})$	$f_{l,a} = \frac{2E_{frp}\varepsilon_{h,rup}t_j}{D}$
Lam and Teng[107]	$f'_{cc} = f'_c(1 + 3.3\frac{f_{l,a}}{f'_c})$	$f_{l,a} = \frac{2E_{frp}\varepsilon_{h,rup}t_j}{D}$
Oliveira et al.[108]	$f'_{cc} = \max\begin{cases} f_{cc1} = f'_c(1 + 0.25(\frac{f_{l,a}}{f'_c})^{0.7}) \\ f_{cc2} = f'_c(0.94 + 0.59(\frac{f_{l,a}}{f'_c})^{0.7}) \\ f_{ccu} = f'_c(0.35 + 3.79(\frac{f_{l,a}}{f'_c})^{0.7}) \end{cases}$	$f_{l,a} = E_l\varepsilon_{h,rup}$ $E_l = \frac{2t_jE_{frp}}{D}$ $k_\varepsilon = 0.861 - 2.51 * 10^{-3}f'_c$ $-0.606 * 10^{-6}E_{frp} + 2.7 * 10^{-5}E_l$

strain has not been considered in models proposed by Wu and Wei,[100] Pham and Hadi,[101] Fahmy and Wu,[102] Youssef et al.,[94] and Kumutha et al.[103]

In this research, the equation of the compressive strength of the FRP-confined concrete with circular section has been considered as follows

$$f'_{cc} = f'_c + \alpha f_{l,a} \tag{7}$$

wherein the actual confinement stress caused by the FRP wrap ($f_{l,a}$) has been considered based on equation (1). Considering the strength of the unconfined concrete, the value of α is found as follows

$$\alpha = \begin{cases} \alpha_1 & f'_c \leq 35\,\text{MPa} \\ \alpha_2 & f'_c > 35\,\text{MPa} \end{cases} \tag{8}$$

Based on the average unconfined compressive strength of the specimens in Table 1, 35 MPa has been selected. In this study, the strain efficiency factor k_ε has been considered as two separate functions (or their combination) which create three separate models for estimating the compressive strength of the FRP-confined concrete. These two functions are the strain ratio (ρ_ε) and effective stiffness ratio (ρ_k) defined as follows

$$\rho_k = \frac{E_{frp}}{f'_c} \tag{9}$$

$$\rho_\varepsilon = \frac{\varepsilon_{frp}}{\varepsilon_{co}} \tag{10}$$

Next, models presented for estimating the compressive strength of the FRP-confined concrete are discussed wherein the FRP strain efficiency factor is considered in three different forms.

Model I: FRP strain efficiency factor as a function of ffective stiffness

In this case, the FRP strain efficiency factor is considered as a function of the stiffness ratio

$$k_\varepsilon = f(\rho_\varepsilon) = \beta_1 + \gamma_1\rho_k^{\lambda_1} \tag{11}$$

Values of α_1 and α_2 in equation (8) and β_1, γ_1, and λ_1 in equation (11) have been so calculated, using the optimization GA, that the difference between the compression strength estimated by the analytical model (equation (7)) and that obtained in the test will be the lowest. Accordingly, α_1, α_2, β_1, γ_1, and λ_1 can be so calculated, using the GA, that the value of Z, calculated by equation (12), reaches its minimum. Therefore, in the optimization algorithm, equation (12) was considered as the optimal function as follows

$$Z = 1 - R^2 + e \tag{12}$$

$$e_{tot} = \frac{\sum\left|(f'_{cc})_{\exp} - (f'_{cc})_{pre}\right|}{\sum\left|(f'_{cc})_{\exp}\right|} \tag{13}$$

In equation (12), R^2 is the correlation coefficient and e_{tot} is the total error. In equation (13) *exp* and *pre* suffixes represent the experimental results and those estimated through the model in equation (7), respectively.

Considering a range 0 to 6 for α_1 and α_2 and -3 to 3 for β_1, γ_1 and λ_1, values of α_1, α_2, β_1, γ_1 and λ_1 were estimated to be 5.2812, 4.4537, 0.4748, -1.9181, and -0.8035, respectively, through optimizing Z (equation (12)) for the test results presented in Table 1. Based on the above procedure, a value of $Z = 0.5694$ was calculated for the optimal function. According to the obtained results, an increase in the effective stiffness ratio increases the strain efficiency factor, meaning that the latter is directly related to the former. Considering the strain efficiency factor as a function of the effective stiffness ratio (equation (11)), the percentage of increase in the compressive strength caused by FRP for a concrete specimen with an unconfined compressive strength less than 35 MPa will be about 19% higher than that the same specimen with an unconfined compressive strength greater than 35 MPa.

Model II: FRP strain efficiency factor as a function of strain ratio

As in previous case, the strain efficiency factor is considered as a function of strain ratio

$$k_\varepsilon = f(\rho_k) = \beta_2 + \gamma_2 \rho_\varepsilon^{\lambda_2} \tag{14}$$

In this study, the strain related to f'_c in an unconfined concrete is calculated as follows[95]

$$\varepsilon_{co} = \frac{f'_c}{E_c} \tag{15}$$

$$E_c = 4700\sqrt{f'_c} \tag{16}$$

For this model too, as mentioned in previous section, values of α_1 and α_2 in equation (8) and β_2, γ_2, and λ_2 are calculated using the optimization GA. Values of α_1, α_2, β_2, γ_2, and λ_2 were calculated to be 3.8522, 3.5525, 0.8992, -0.0594, and 0.7936, respectively through optimizing test specimens in Table 1 with an initial population of 10,000 after 100 iterations and considering a range 0 to 6 for α_1 and α_2, and -3 to 3 for β_2, γ_2, and λ_2. The value of the optimal function calculated using equation (12) for 662 specimens used in optimization is equal to 0.5019. An increase in the strain ratio increases the strain efficiency factor; therefore, the two are directly related. In this case, the percentage of increase in the confined compressive strength for the concrete with an unconfined strength less than 35 MPa is 8% higher than that greater than 35 MPa (11% less than model I). A comparison of the optimal functions in models I and II showed that the effect of strain ratio in the model II that estimates the compressive strength of FRP-confined columns is greater and reduces the optimal function by about 13% compared to model I.

Model III: FRP strain efficiency factor as a combinatory function of strain ratio (ρε) and effective stiffness ratio (ρk)

Finally, the FRP strain efficiency factor is considered as a combinatory function of the strain ratio and effective stiffness ratio as follows

$$k_\varepsilon = f(\rho_k) = \beta_3 + \gamma_3 \rho_k^{\lambda_3} + \delta_3 \rho_\varepsilon^{\varphi_3} + \theta_3 \rho_\varepsilon^{\eta_3} \rho_k^{\zeta_3} \tag{17}$$

For this model, values of α_1 and α_2 in equation (8) and β_3, γ_3, λ_3, δ_3, φ_3, θ_3, η_3, and ξ_3 are calculated using the optimization GA as mentioned in previous sections. Values of α_1, α_2, β_3, γ_3, λ_3, δ_3, φ_3, θ_3, η_3, and ξ_3 were estimated to be 3.499, 3.0481, 0.2071, 1.4729, -0.0815, -0.0305, 1.0841, 0.0045, 20, and -7.1945, respectively through optimizing test specimens in Table 1 with an initial population of 10,000 after 100 iterations and considering a range 0 to 6 for α_1 and α_2, and -20 to 20 for β_3, γ_3, λ_3, δ_3, φ_3, θ_3, η_3, and ξ_3. The value of the optimal function calculated using equation (12) for 662 specimens used in optimization is equal to 0.4885 and results show that when the combination of the two ratios is used, the optimal function reduces by 17 and 3% compared to models I and II, respectively.

Evaluation of proposed models

To evaluate the proposed models, some additional experimental data have been used from other studies and presented in Table 3. As seen, the total number of specimens used in this table is 70.

Based on equation (12), the total error, e_{tot}, for each model has been calculated and presented in Table 4. For a better comparison, the model performance is evaluated through such statistical indices as: (1) mean square error, (2) average absolute error, and (3) standard deviation determined by equations (18) to (20), respectively. These indexes, calculated for both the modeling specimens in Table 1, and the evaluating specimens in Table 3, are outlined in Table 4.

As shown, considering the statistical results, the proposed models have less error compared to other models. Models I, II, and III have averagely reduced the total error for all the specimens in Tables 1 and 3 by 21.9, 24.1 and 21.6%, respectively, compared to the models proposed by Wu and Wei,[100] Pham and Hadi,[101] Ozbakkaloglu and Lim,[104] Fahmy and Wu,[102] Teng et al.,[105] Youssef et al.,[94] Kumutha et al.,[103] Guralnick and Gunawan,[106] and Lam and Teng.[107]

Figure 3(a) to (m) shows the performance of the models proposed by Wu and Wei,[100] Pham and Hadi,[101] Ozbakkaloglu and Lim,[104] Fahmy and Wu,[102] Teng et al.,[105] Youssef et al.,[94] Kumutha et al.,[103] Guralnick and Gunawan,[106] and Lam and Teng,[107] and proposed models I, II, and III for all the specimens in Tables 1 and 3 (732 specimens). As shown, the proposed models estimate the compressive strength of the FRP-confined, circular section concrete specimens better.

For more comparisons, the values of optimal functions, that involve the effects of the total error and correlation coefficient, are provided in Table 5 for all the models studied in this research (732 specimens). And to check the effects of the proposed models, percent reductions created by all three models compared to other mentioned models are given in Table 5.

In Table 5, a negative/positive sign indicates a decrease/an increase in the value of the optimal function compared to other mentioned models. Results in Table 5 show that models II and III perform better, but

Table 3. Details of the FRP-confined circular concrete specimens for evaluating procedure.

Reference	Total number of database	Diameter (mm)	Unconfined concrete strength range (MPa)	FRP type
Abdollahi et al.[109]	5	150	14.8–41.7	GFRP
Almusallam[110]	4	150	47.7–50.8	GFRP
Howie and Karbhari[111]	12	152	38.6	GFRP
Ilki et al.[112]	12	150	6.2	CFRP
Issa and Karam[113]	9	150	30.5	CFRP
Lin and Chen[114]	10	120	32.7	GFRP, HM-CFRP
Lin and Liao[115]	6	100	23.9	CFRP
Miyauchi et al.[116]	6	100–150	23.6–26.3	CFRP
Vincent and Ozbakkaloglu[117]	6	152	49.4	AFRP

Table 4. Statistical indicators for FRP-confined circular concrete specimens.

Theoretical models	Specimens of Table 1				Specimens of Table 3			
	MSE	*AAE*	*SD*	e_{tot}	*MSE*	*AAE*	*SD*	e_{tot}
Wu and Wei[100]	8.06	17.15	28.26	17.37	1.66	10.17	12.99	9.35
Pham and Hadi[101]	5.58	16.9	23.67	17.14	2.29	11.96	15.16	11.84
Ozbakkaloglu and Lim[104]	6.52	17.43	25.66	17.62	2.21	11.62	15.03	11.86
Fahmy and Wu[102]	4.61	17.27	21.08	19.44	3.17	15.45	15.76	16.77
Teng et al.[105]	6.98	18.92	24.54	19.87	2.47	13.03	10.79	12.8
Youssef et al.[94]	12.94	19.47	35.81	20.3	5.76	18.79	24.15	19.8
Kumutha et al.[103]	10.17	28.27	18.05	31.49	12.65	32.59	15.12	34.61
Guralnick and Gunawan[106]	6	17.7	23.75	17.18	2.79	12.26	16.89	11.68
Lam and Teng[107]	6.31	17.35	25.18	18.6	1.83	11.61	12.26	11.53
Oliveira et al.[108]	8.71	17.79	28.72	17.85	2.05	11.02	14.2	10.39
Model I	7.89	16.01	28.14	16.2	1.79	11.27	13.52	11.33
Model II	6.36	15.48	25.27	15.8	2.47	12.5	14.66	12.38
Model III	5.8	15.5	24.15	15.72	5.19	16.73	21.28	16.71

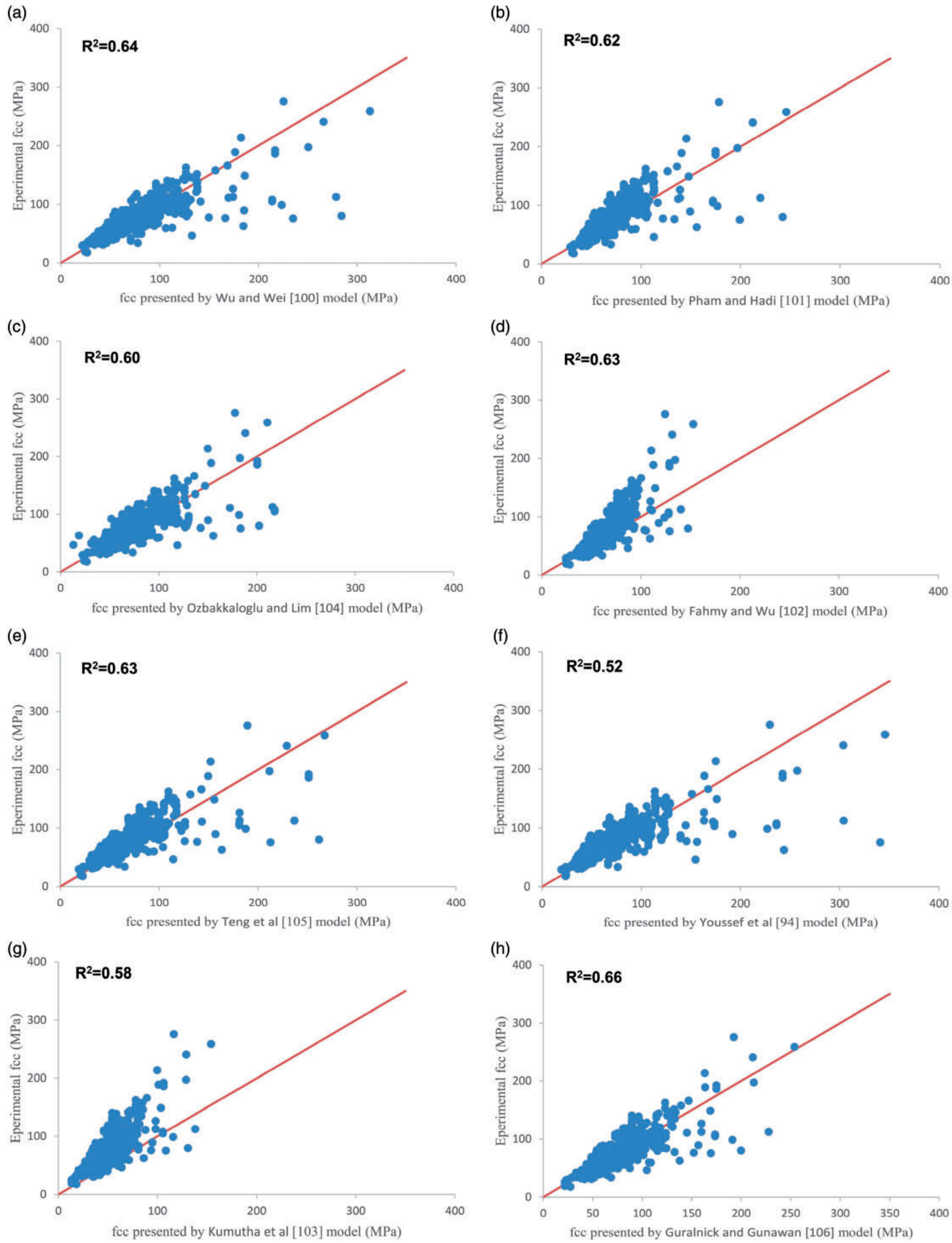

Figure 3. Performance of the selected models in comparison with experimental data: a) Ref. [100], b) Ref. [101], c) Ref. [104], d) Ref. [102], e) Ref. [105], f) Ref. [94], g) Ref. [103], h) Ref. [106], i) Ref. [107], J) Ref. [108], k) the proposed model I, l) the proposed model II and m) the proposed model III.

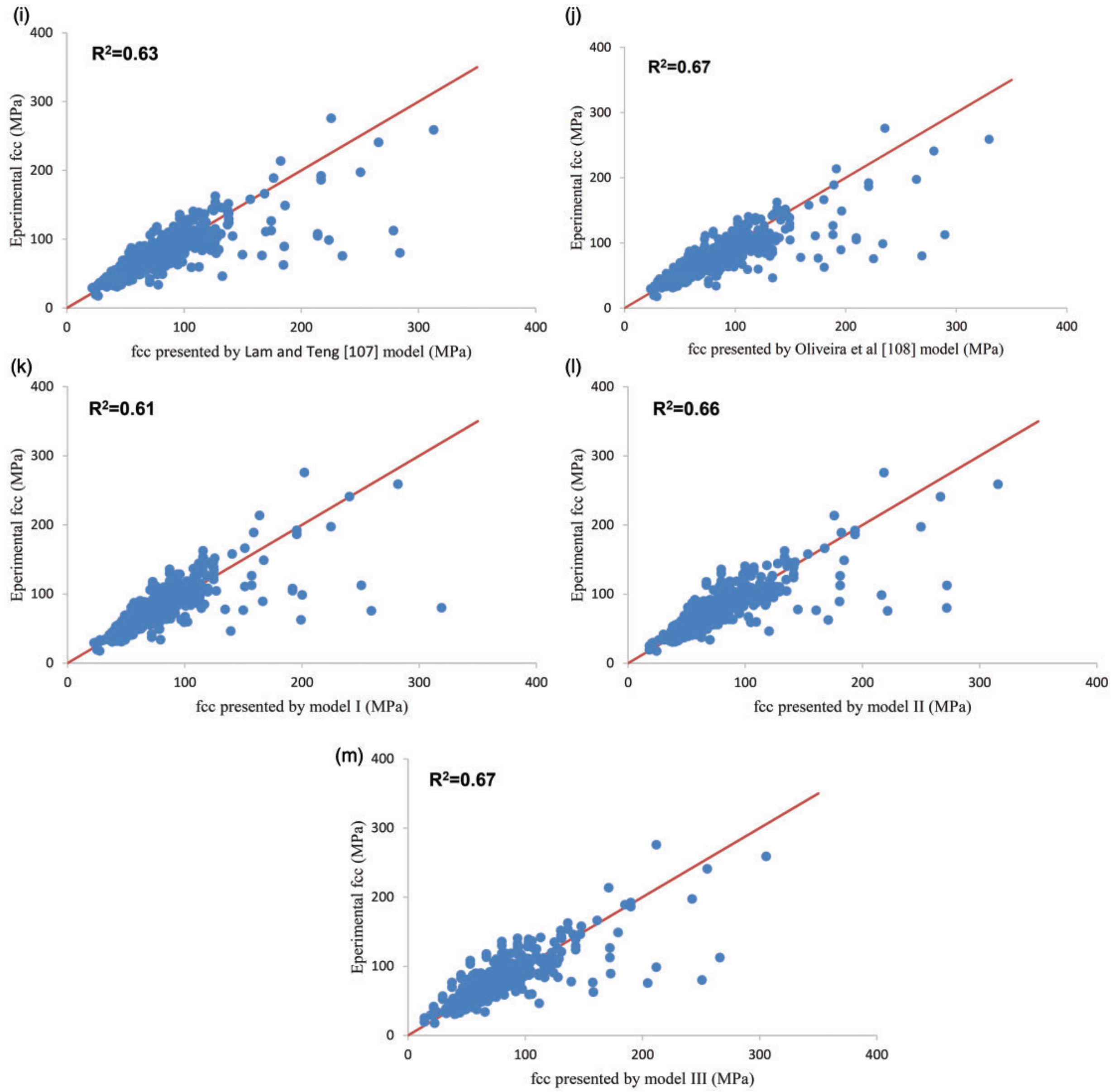

Figure 3. Continued

Table 5. Comparison of optimal function for models.

Theoretical model	Z	Percent increase/ decrease model I	Percent increase/ decrease model II	Percent increase/ decrease model III
Wu and Wei[100]	0.51	6.21	−5.24	−5.43
Pham and Hadi[101]	0.54	1.93	−10.03	−10.24
Ozbakkaloglu and Lim[104]	0.56	−2.01	−14.46	−14.67
Fahmy and Wu[102]	0.55	−0.63	−12.92	−13.13
Teng et al.[105]	0.55	−0.74	−13.04	−13.25
Youssef et al.[94]	0.68	−23.94	−39.07	−39.33
Kumutha et al.[103]	0.73	−32.52	−48.70	−48.98
Guralnick and Gunawan[106]	0.50	8.80	−2.33	−2.52
Lam and Teng[107]	0.54	0.50	−11.64	−11.84
Oliveira et al.[108]	0.50	9.76	−1.26	−1.44

it should be noted that their accuracies do not differ much. According to this table, models I, II, and III averagely reduce the value of the optimum function by 3.2, 15.9, and 16.1%, respectively, compared to other models mentioned in this study.

Conclusions

In this study, three models have been proposed for estimating the compressive strength of FRP-confined, circular-section columns. The strain efficiency factor of FRP in these models has been considered as: (i) a function of the strain ratio, (ii) a function of the effective stiffness ratio, and (iii) a function of the combination of these ratios. Results from this research are shown as follows:

1. Compared to the effective stiffness ratio, the effect of the strain ratio for estimating the compressive strength of confined circular columns is greater.
2. Models proposed in this research estimate the compressive strength of circular columns confined with different types of FRP better; the three proposed models averagely reduce the total error by 21.9, 24.1, and 21.6% and values of the optimal function by 3.2, 15.9, and 16.1% compared to the models mentioned in this study.
3. There is not much difference between the value of the optimal function (which is a combination of total error and correlation coefficient) of the model wherein the FRP strain efficiency factor is a function of the strain ratio and that of the one wherein FRP strain efficiency factor is a function of the combination of the strain ratio and the effective stiffness ratio. Therefore, considering the convenience of the model wherein the FRP strain efficiency factor is a function of the strain ratio, it can be selected as the optimal model.

Declaration of conflicting interests

The author(s) declared no potential conflicts of interest with respect to the research, authorship, and/or publication of this article.

Funding

The author(s) received no financial support for the research, authorship, and/or publication of this article.

ORCID iD

Yaser Moodi https://orcid.org/0000-0002-3763-1629

References

1. Fam AZ and Rizkalla SH. Behavior of axially loaded concrete-filled circular fiber-reinforced polymer tubes. *ACI Struct J* 2001; 98: 280–289.
2. Teng JG, Chen JF, Smith ST, et al. *FRP strengthened RC structures*. New York: John Wiley & Sons, 2001.
3. Becque J, Patnaik AK and Rizkalla SH. Analytic models for concrete confined with FRP tubes. *ASCE J Compos Constr* 2003; 7: 31–38.
4. Nanni A and Bradford NM. FRP jacketed concrete uniaxial compression. *Constr Build Mater* 1995; 9: 115–124.
5. Fardis MN and Khalili HH. FRP-encased concrete as a structural material. *Mag Concr Res* 1982; 34: 191–202.
6. Mander JB, Priestley MJN and Park R. Theoretical stress–strain model for confined concrete. *J Struct Eng* 1988; 114: 1804–1826.
7. ACI 440.2R-02. *Guide for the design and construction of externally bonded FRP systems for strengthening concrete structures*. Farmington: American Concrete Institute, 2002.
8. Lam L and Teng JG. Design-oriented stress–strain model for FRP-confined concrete. *Constr Build Mater* 2003; 17: 471–489.
9. Sadeghian P and Fam A. Improved design-oriented confinement models for FRP-wrapped concrete cylinders based on statistical analyses. *Eng Struct* 2015; 87: 162–182.
10. Moodi Y, Farahi Shahri S and Mousavi SR. Providing a model for estimating the compressive strength of square and rectangular columns confined with a variety of fibre-reinforced polymer sheets. *J Reinforc Plast Compos* 2017; 36: 1602–1612.
11. Moodi Y, Mousavi SR, Ghavidel A, et al. Using response surface methodology and providing a modified model using whale algorithm for estimating the compressive strength of columns confined with FRP sheets. *Constr Build Mater* 2018; 183: 163–170.
12. Lim JC and Ozbakkaloglu T. Hoop strains in FRP-confined concrete columns: experimental observations. *Mater Struct* 2015; 48: 2839–2854.
13. Ahmad SH, Khaloo AR and Irshaid A. Behavior of concrete spirally confined by fiberglass filaments. *Mag Concr Res* 1991; 43: 143–148.
14. Aire C, Gettu R, Casas JR, et al. Concrete laterally confined with fibre-reinforced polymers (FRP): experimental study and theoretical model. *Mater Construc* 2010; 60: 19–31.
15. Akogbe RK, Wu ZM and Liang M. Size effect of axial compressive strength of CFRP confined concrete cylinders. *Int J Concr Struct Mater* 2011; 5: 49–55.
16. Al-Salloum Y and Siddiqui N. Compressive strength prediction model for FRP confined concrete. In: *Proceedings of the 9th international symposium on FRP reinforcement for concrete structures*, Sydney, Australia, 2009.
17. Au C and Buyukozturk O. Effect of fiber orientation and ply mix on fiber reinforced polymer-confined concrete. *J Compos Constr* 2005; 9: 397–407.

18. Benzaid R, Mesbah H and Chikh NE. FRP-confined concrete cylinders: axial compression experiments and strength model. *J Reinforc Plast Compos* 2010; 29: 2469–2488.
19. Berthet JF, Ferrier E and Hamelin P. Compressive behavior of concrete externally confined by composite jackets. Part A: experimental study. *Constr Build Mater* 2005; 19: 223–232.
20. Bisby L, Take WA and Caspary A. Quantifying strain variation FRP confined using digital image correlation proof of concept and initial result. In: *1st Asia-Pacific conference on FRP in structures*, Hong Kong, China, 2007, pp. 599–604
21. Bisby LA, Chen JF, Li SQ, et al. Strengthening fire-damaged concrete by confinement with fibre-reinforced polymer wraps. *Eng Struct* 2011; 33: 3381–3391.
22. Bullo S. Experimental study of the effect the ultimate strain of fiber reinforced plastic jackets on the behavior of confined concrete. In: *Proceedings of the international conference composites in constructions*, Cosenza, Italy, 2003.
23. Carnpione G, Miraglia N and Scibilia N. Compressive behavior of R.C. members strengthened with carbon fiber reinforced plastic layers. *Trans Built Environ* 2001; 57: 397–406.
24. Carey SA and Harries KA. Axial behavior and modeling of confined small-, medium-, and large-scale circular sections with carbon fiber-reinforced polymer jackets. *ACI Struct J* 2005; 102: 596–604.
25. Comert M, Goksu C and Ilki A. Towards a tailored stress-strain behaviour for FRP confined low strength concrete. In: *Proceedings of the 9th international symposium on fiber reinforced polymer reinforcement for concrete structures*, Sydney, Australia, 2009.
26. Cui C and Sheikh SA. Experimental study of normal- and high-strength concrete confined with fiber-reinforced polymers. *J Compos Constr* 2010; 14: 553–561.
27. Hosotani K, Kawashima K and Hoshikuma J. A model for confinement effect for concrete cylinders confined by carbon fiber sheets. *In: Workshop on earthquake engineering frontiers in transportation facilities state*, University of New York, Buffalo, 1997.
28. Ilki A, Kumbasar N and Kov V. Strength and deformability of low strength concrete confined by carbon fiber composite sheets. In: *Proceedings 15th engineering mechanics conference*, New York, USA, 2002.
29. Issa CA. The effect of elevated temperatures on CFRP wrapped concrete cylinders. In: *Proceeding 8th international symposium on fiber reinforcement for concrete structures*, Patras, Greece, 2008.
30. Rochette P and Labossière P. Axial testing of rectangular column models confined with composites. *ASCE J Compos Constr* 2000; 4: 129–136.
31. Jiang T and Teng JG. Analysis-oriented stress–strain models for FRP-confined concrete. *Eng Struct* 2007; 29: 2968–2986.
32. Miyauchi K, Nishibayashi S and Inoue S. Estimation of strengthening effects with carbon fiber sheet for concrete column. In: *3rd International symposium of non-metalic reinforcement for concrete structures*, Canada, 1997.
33. Modarelli R, Micelli F and Manni O. FRP confinement of hollow concrete cylinders and prisms. In: *Proceeding 7th international symposium on fiber reinforced polymer reinforcement of reinforced concrete structures*, Kansas City, USA, 2005.
34. Ongpeng JMC. Retrofitting RC circular columns using CFRP sheet as confinement. In: *Symposium on infrastructure development and the environment*, Diliman, Quezon City, 2006.
35. Owen LM. *Stress-strain behavior of concrete confined by carbon fiber jacketing*. Masters Thesis, University of Washington, Seattle, 1998.
36. Ozbakkaloglu T and Akin E. Behavior of FRP-confined normal- and high-strength concrete under cyclic axial compressive. *J Compos Constr* 2013; 16: 451–463.
37. Picher F, Rochette P and Labossiere P. Confinement of concrete cylinders with CFRP. In: *Proceeding in international conference on composites in infrastructure*, Tuscon, Arizona, 1996.
38. Piekarczy J, Piekarczy W and Blazewichz S. Pressure strength of concrete cylinders reinforced with carbon fiber laminate. *Constr Build Mater* 2011; 25: 2365–2369.
39. Valdmanis V, De Lorenzis L, Rousakis T, et al. Behavior and capacity of CFRP confined concrete cylinder subjected to monotonic and cyclic axial compressive loads. *Struct Concr* 2007; 8: 187–200.
40. Li G, Maricherla D, Singh K, et al. Effect of fiber orientation on the structural behavior of FRP wrapped concrete cylinder. *Compos Struct* 2006; 74: 475–483.
41. Liang M, Wu Z, Ueda T, et al. Experiment and modeling on axial behavior of carbon fiber reinforced polymer confined concrete cylinders with different size. *J Reinforc Plast Compos* 2012; 31: 389–403.
42. Lin HJ and Liao CI. An effective peak stress formula for concrete confined with carbon fiber reinforced plastics. *Can J Civ Eng* 2003; 30: 882–889.
43. Mandal S, Hoskin A and Fam A. Influence of concrete strength on confinement effectiveness of fiber reinforced polymer circular jackets. *ACI Struct J* 2005; 102: 383–392.
44. Mastrapa JC. *Effect of construction bond on confinement with fiber composites*. Masters Thesis, University of Central Florida, Orlando, 1997.
45. Rousakis T. Experimental investigation of concrete cylinders confined by carbon FRP sheet under monotonic and cyclic axial compressive load. Research Report, Chalmers University of Thecknology, Gotenborg, Sweden, 2001.
46. Rousakis T, You C, De Lorenzis L, et al. Concrete cylinder confined by carbon FRP sheet subjected to monotonic and cyclic axial compressive loads. In: *6th International Symposium on FRP Reinforcement for Concrete Structures*, Singapore, 2003, pp. 571–580.
47. Saenz N and Pantelides CP. Short and medium term durability evaluation of FRP confined circular concrete. *J Compos Constr* 2006; 10: 244–253.
48. Santaros D, Filho AC, Beber AJ, et al., Concrete columns confined with CFRP sheet. In: *Proceeding international conference of FRP composites in civil engineering*, Hong Kong, 2001.

49. Shahawy M, Mirmiran A and Beitelman T. Tests and modeling of carbon wrapped concrete columns. *Compos B Eng* 2000; 31: 471–480.
50. Shao Y, Zhu Z and Mirmiran A. Cyclic modeling of FRP confined concrete with improved ductility. *Cem Concr Compos* 2006; 2: 956–968.
51. Wu G, Wu ZS, Lu ZT, et al. Structural performance of concrete confined with hybrid FRP composites. *J Reinforc Plast Compos* 2008; 27: 1323–1348.
52. Wu H, Wang Y, Yu L, et al. Experimental and computational studies on high strength concrete circular columns confined by aramid fiber reinforced polymer sheet. *J Compos Constr* 2009; 13: 125–134.
53. Xiao Y and Wu H. Compressive behavior concrete confined by carbon fiber composites jackets. *J Mater Civ Eng* 2000; 12: 139–146.
54. Karabinis AI and Rousakis TC. Concrete confined by FRP material: a plasticity approach. *ASCE Eng Struct* 2002; 24: 923–932.
55. Karam GN and Tabbara M. Corner effects in CFRP-wrapped square columns. *Mag Concr Res* 2004; 56: 461–464.
56. Karantzikis M, Papanicolaou CG, Antonopoulos CP, et al. Experimental investigation of nonconventional confinement for concrete using FRP. *J Compos Constr* 2005; 9: 480–487.
57. Karbhari VM and Gao Y. Composite jacketed concrete under uniaxial compression – verification of simple design equations. *J Mater Civ Eng* 1997; 9: 185–193.
58. Kono S, Inazuni M, Kaku T. Evaluation of confining effects of CFRP sheets on reinforced concrete members. In: *2nd International conference, Composites in infrastructure*, Tucson, 1998, pp. 343–355.
59. Lam L and Teng G. Ultimate condition of FRP confined concrete. *J Compos Constr* 2004; 8: 539–548.
60. Lam L, Teng JG, Cheung CH, et al. FRP-confined concrete under axial cyclic compression. *Cem Concr Compos* 2006; 28: 949–958.
61. Lee J, Yi C, Jeong H, et al. Compressive response of concrete confined with steel spirals and FRP composites. *J Compos Mater* 2009; 44: 481–504.
62. Dai JG, Bai YL and Teng JG. Behavior and modeling of concrete confined with FRP composites of large deformability. *J Compos Constr* 2011; 15: 963–973.
63. Demers M and Neale KW. Strengthening of concrete columns with unidirectional composite sheets. In: *Proceedings of developments in short and medium span bridge engineering*, Montreal, Canada, 1994.
64. Elsanadedy HM, Al-Salloum YA, Alsayed SH, et al. Experimental and numerical investigation of size effects in FRP-wrapped concrete columns. *Constr Build Mater* 2012; 29: 56–72.
65. Erdil BU, Akyuz U and Yaman IO. Mechanical behavior of CFRP confined low strength concretes subjected to simultaneous heating-cooling cycles and sustained loading. *Mater Struct* 2012; 45: 223–233.
66. Evans J, Kocman M and Kretschmer T. *Hybrid FRP confined concrete columns*. Adelaide: The School of Civil, Environmental and Mining Engineering, University of Adelaide, 2008.
67. Green MF, Bisby LA, Fam AZ, et al. FRP confined concrete column: behavior under extreme conditions. *Cem Concr Compos* 2006; 28: 928–993.
68. Harmon TG and Slattery KT. Advanced composite confinement of concrete. In: *Proceedings advanced composite materials for bridges and structures*, Montreal, Canada, 1992.
69. Harries KA and Carey A. Shape and "gap" effects on the behavior of variably confined concrete. *Cement Concr Res* 2003; 33: 881–889.
70. Harries KA and Kharel G. Behavior and modeling of concrete subject to variable confining pressure. *ACI Mater J* 2002; 99: 180–189.
71. Matthys S, Taerwe L and Audenaert K. Tests on axially loaded concrete columns confined by fiber reinforced polymer sheets wrapping. In: *Proceedings of the 4th international symposium on fiber reinforced polymer reinforcement for concrete structures*, 1999, pp. 217–228.
72. Micelli F, Myers JJ and Murthy S. Effect of environmental cycles on concrete cylinders confined with FRP. In: *Proceeding international conference on composite in construction*, Porto, Portugal, 2001.
73. Mirmiran A, Shahawy M, Samaan M, et al. Effects of column parameters on FRP confined concrete. *J Compos Constr* 1998; 2: 175–185.
74. Shehata Iaem Carneiro LAV and Shehata L. Strength of short concrete columns confined with CFRP sheet. *Mat Struct* 2002; 35: 50–58.
75. Shehata Iaem Carneiro LAV and Shehata LCD. Strength of confined short concrete Columns. In: *Proceeding 8th international symptom on fiber reinforcement for concrete structures*, Patras, Greece, 2007.
76. Silva MAG and Rodrigues CC. Size and relative stiffness effects on compressive failure of concrete columns wrapped with glass FRP. *J Mater Civ Eng* 2006; 18: 334–342.
77. Smith ST, Kim SJ and Zhang H. Behavior and effectiveness of FRP wrap in the confinement of large concrete cylinders. *J Compos Constr* 2010; 14: 573–582.
78. Song X, Gu X, Li Y, et al. Mechanical behavior of FRP strengthened concrete columns subjected toconcentric and eccentric compression loading. *J Compos Constr* 2013; 17: 336–346.
79. Stanton JF and Owen LM. Influence of concrete strength and confinement type on the response of FRP confined concrete cylinders. *ACI Spec Publ* 2006; 238: 347–362.
80. Suter R and Pinzelli R. Confinement of concrete columns with FRP sheet. In: *Proceeding 5th symposium on fiber reinforcement plastic reinforcement for concrete structure*, London, 2001.
81. Tamuzs V, Valdmins V, Tepfer R, et al. Stability analysis of CFRP wrapped concrete columns strengthened with external longitudinal CFRP sheet. *Mech Compos Mater* 2008; 44: 199–208.

82. Teng JG, Yu T, Wong YL, et al. Hybrid FRP concrete steel tubular columns: concept and behavior. *Constr Build Mater* 2007; 21: 846–854.
83. Thériault M, Neale KW and Claude S. Fiber reinforced polymer confined circular concrete columns: investigation of size and slenderness effects. *J Compos Constr* 2004; 8: 323–331.
84. Vincent T and Ozbakkaloglu T. Influence of concrete strength and confinement method on axial compressive behavior of FRP confined and Ultra high strength concrete. *Compos B Eng* 2010; 50: 413–428.
85. Wang LM and Wu YF. Effect of corner radius on the performance of CFRP-confined square concrete columns: test. *Eng Struct* 2008; 30: 493–505.
86. Wang Y and Wu HL. Size effect of concrete short columns confined with aramid FRP jacket. *J Compos Constr* 2011; 15: 535–544.
87. Wu YF and Jiang JF. Effective strain of FRP confined circular concrete columns. *Compos Struct* 2013; 95: 479–491.
88. Wang Y and Zhang D. Creep-effect on mechanical behavior of concrete confined by FRP under axial compression. *J Eng Mech* 2009; 135: 1315–1322.
89. Watanabe K, Nakamura R, Honda Y, et al. Confinement effect of FRP sheet on strength and ductility of concrete cylinders under uniaxial compression. In: *3rd International symposium, Non-metallic (FRP) reinforcement for concrete structures*, Sapporo, Japan, 1997, pp. 233–238.
90. Wong YL, Yu T, Teng JG, et al. Behavior of FRP-confined concrete in annular section columns. *Compos B Eng* 2008; 39: 451–466.
91. Wu YF and Jiang C. Effect of load eccentricity on the stress-strain relationship of FRP confined concrete columns. *Compos Struct* 2013; 98: 228–241.
92. Wu G, Lü ZT and Wu ZS. Strength and ductility of concrete cylinders confined with FRP composites. *Constr Build Mater* 2006; 20: 134–148.
93. Yan Z, Pantelides CP and Reaveley D. Fiber reinforced polymer jacketed and shape modified compression member: I-experimental behavior. *ACI Struct J* 2006; 6: 885–893.
94. Youssef MN, Feng MQ and Mosallam AS. Stress–strain model for concrete confined by FRP composites. *Compos B Eng* 2007; 38: 614–628.
95. Zhang S, Ye L and Mai YW. Study on polymer composite strengthening systems for concrete columns. *Appl Compos Mater* 2000; 7: 125–138.
96. Salar M, Ghasemi MR and Dizangian B. A fast GA-based method for solving truss optimization problems. *Int J Optim Civil Eng* 2016; 6: 101–114.
97. Salar M, Ghasemi MR and Dizangian B. Practical optimization of deployable and scissor-like structures using a fast GA method. *Front Struct Civ Eng* 2018; 13: 557–568.
98. Rao MA, Srinivas J and Murthy B. Damage detection in vibrating bodies using genetic algorithms. *Comput Struct* 2016; 82: 963–968.
99. Cheng M and Runwei C. *Genetic algorithms and engineering optimization*. New York: Wiley-Interscience, 2000.
100. Wu YF and Wei Y. General stress-strain model for steel- and FRP-confined concrete. *J Compos Constr* 2015; 19: 04014069-1–04014069-14.
101. Pham TM and Hadi M. Confinement model for FRP confined normal- and high-strength concrete circular columns. *Constr Build Mater* 2014; 69: 83–90.
102. Fahmy MFM and Wu Z. Evaluating and proposing models of circular concrete columns confined with different FRP composites. *Compos B Eng* 2010; 41: 199–213.
103. Kumutha R, Vaidyanathan R and Palanichamy MS. Behaviour of reinforced concrete rectangular columns strengthened using GFRP. *Cem Concr Compos* 2007; 29: 609–615.
104. Ozbakkaloglu T and Lim JC. Axial compressive behavior of FRP-confined concrete: experimental test database and a new design-oriented model. *Compos B Eng* 2013; 55: 607–634.
105. Teng JG, Jiang T, Lam L, et al. Refinement of a design-oriented stress–strain model for FRP-confined concrete. *J Compos Constr* 2009; 13: 269–278.
106. Guralnick SA and Gunawan L. Strengthening of reinforced concrete bridge columns with FRP wrap. *Pract Period Struct Des Constr* 2005; 11: 218–228.
107. Lam L and Teng JG. Design-oriented stress-strain model for FRP-confined concrete in rectangular columns. *J Reinforc Plast Compos* 2003; 22: 1149–1186.
108. De Oliveira DS, Raiz GEV and Carrazedo R. Experimental study on normal-strength, high-strength and ultrahigh-strength concrete confined by carbon and glass FRP laminates. *J Compos Constr* 2019; 23: 04018072-1–04018072-15.
109. Abdollahi B, Bakhshi M and Shekarchi M. Experimental modeling of GFRP confined concrete cylinders subjected to axial loads. In: *Proceedings of the 8th international symposium on FRP reinforcement for concrete structures*, Patras, Greece, 2007.
110. Almusallam TH. Behavior of normal and high-strength concrete cylinders confined with E-glass/epoxy composite laminates. *Compos B Eng* 2007; 38: 629–639.
111. Howie I and Karbhari VM. Effect of materials architecture on strengthening efficiency of composite wraps for deteriorating columns in the north-east. In: *3rd Materials engineering conference*, San Diego, CA, USA 1994.
112. Ilki A, Kumbasar N and Kov V. Low strength concrete members externally confined with FRP sheet. *Struct Eng Mech* 2004; 18: 167–194.
113. Issa CA and Karam GN. Compressive strength of concrete cylinders with variable widths CFRP wraps. In: *Proceeding 4th international conference on advanced composite materials in bridges and structures*, Calgary, Canada, 2004.
114. Lin HJ and Chen CT. Strength of concrete cylinder confined by composite materials. *J Reinforc Plast Compos* 2001; 20: 1577–1600.

115. Lin HJ and Liao CI. Compressive strength of reinforced concrete column confined by composite material. *Compos Struct* 2004; 65: 239–250.
116. Miyauchi K, Inoue S, Kuroda, et al. Strengthening effects of concrete column with carbon fiber sheet. *Transactions of the Japan Concrete Institute* 1999; 21: 143–150.
117. Vincent T and Ozbakkaloglu T. Influence of fiber orientation and specimen end condition on axial compressive behavior of FRP confined concrete. *Constr Build Mater* 2013; 47: 814–826.